

Preferential CO oxidation in the presence of H₂, H₂O and CO₂ at short contact-times

A. Jhalani and L.D. Schmidt*

Department of Chemical Engineering and Materials Science, University of Minnesota, 421 Washington Ave. SE, Minneapolis, MN, 55455 USA

Received 13 May 2005; accepted 11 July 2005

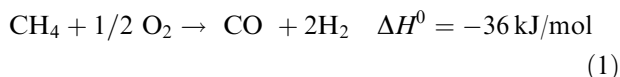
High selectivities and conversions in the preferential oxidation of CO in the presence of large quantities of H₂, H₂O and CO₂ are demonstrated on noble metal catalysts at millisecond contact times (~10–15 ms) for temperatures between 150 and 500 °C. With a simulated water-gas shift product stream containing 0.5% CO and varying amounts of H₂, H₂O and CO₂, we are able to achieve ~90% CO conversions on a Ru catalyst at temperatures of ~300 °C using a stoichiometric amount of O₂ (0.25%). Experiments with and without O₂ and with varying H₂O reveal that significant water-gas shift occurs on Pt and Pt-ceria catalysts at temperatures between 250 and 400 °C, while significant CH₄ is formed on Ru and Rh catalysts at temperatures greater than 250 and 350 °C, respectively. The presence of H₂O blocks H₂ adsorption and allows preferential CO oxidation at higher temperatures where rates are high. We propose that a multistage preferential oxidation reactor using these catalysts can be used to bring down CO content from 5000 ppm at the reactor entrance to less than 100 ppm at very short contact-times.

KEY WORDS: preferential oxidation (PROS); water-gas shift (WGS); methanation (MR); partial oxidation; short contact-times; Ru; Rh.

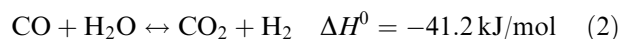
1. Introduction

The use of PEM fuel cells requires the production of pure H₂ with no more than ~10 ppm CO [1]. CO-free H₂ generation on board a fuel cell-powered vehicle using existing fuels like compressed natural gas and gasoline is emerging as the technology of choice because it utilizes existing infrastructure and avoids H₂ storage on board the vehicle. It is now agreed that such a H₂ production system will involve a combination of three different reactions steps in series: partial oxidation (POX), water-gas shift (WGS) and preferential oxidation (PROX) [1–3]. Each of these conventionally requires a separate reactor with ~1 s residence time.

A possible integrated short contact-time H₂ generation reactor along with the proposed temperature profile in the reactor is sketched in figure 1(a). Panel (b) shows the possible mole fraction profiles of different species expected in our reactor. In the first stage, the hydrocarbon fuel is converted to syngas (or synthesis gas, a mixture of CO and H₂) by oxidation under oxygen deficient conditions using POX



In the second stage, a large portion of the CO in the syngas stream is converted to CO₂ and H₂ using the WGS reaction



The remaining CO in the product stream is then selectively oxidized in the preferential oxidation (PROX) reaction



Research in our laboratory over the past decade has focused on POX of hydrocarbons on noble metal catalysts at millisecond contact-times [4–7]. It has been demonstrated that >90% fuel conversion and >90% syngas selectivity can be achieved for a large number of fuels such as methane [4], decane [5,7], ethanol [6], etc. The study of WGS on noble metals has shown that high CO conversions (>90%) can be achieved in this stage at very short contact-times of ~50 ms [8].

In this paper, we investigate the potential of high-temperature, short contact-time PROX of CO on noble metal catalysts using a simulated WGS product stream. The long-term application of this research is an integrated staged reactor, and we simulate this using feeds and conditions that would be required for the application.

In figure 2(a) and (b) are shown calculated equilibrium mole fractions of different species as a function of temperature, with and without CH₄ in the product stream, respectively. Three different zones are marked to show the approximate temperature range in which POX, WGS and PROX would occur in an integrated reactor. The feed for figure 2(a) consists of CH₄, O₂, H₂O and N₂ with C/O=0.75 and a steam/carbon=4 while CH₄ and O₂ were replaced by CO, CO₂ and H₂ for calculations in figure 2(b). Although the equilibrium CO mole fraction goes to zero for both the cases at low temperatures, little H₂ and significant CH₄ are formed at

* To whom correspondence should be addressed.
E-mail: schmidt@cems.umn.edu

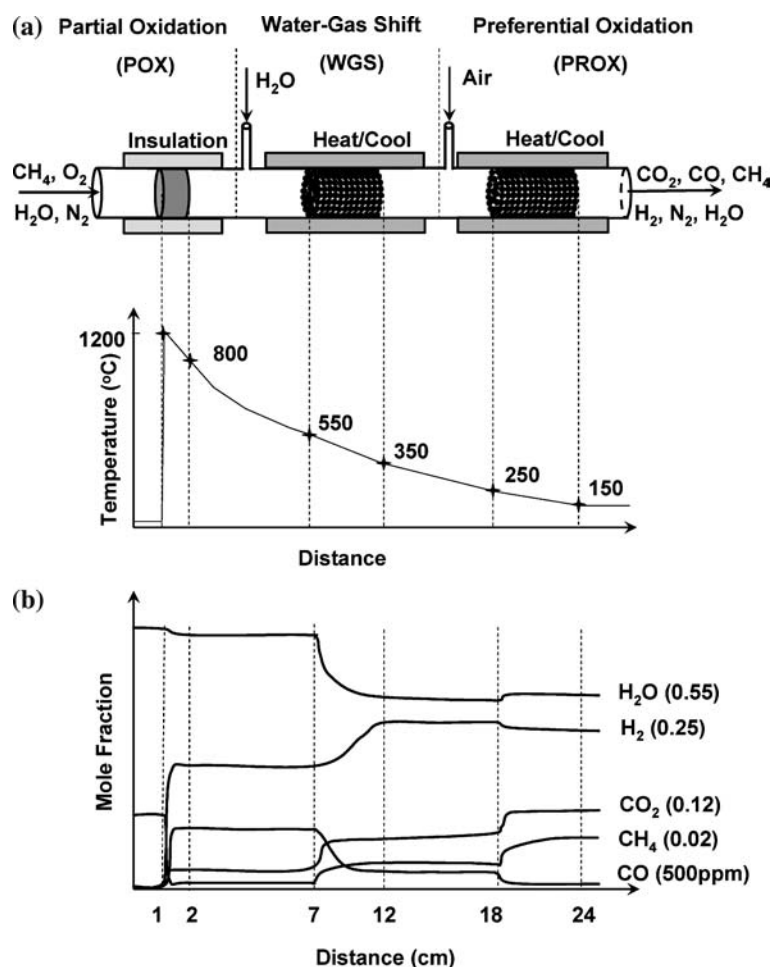


Figure 1. (a) An integrated H_2 generation reactor combining POX, WGS and PROX along with the proposed temperature profile for integrated reactor; (b) approximate mole fraction profiles of different species in our reactor. The mole fractions do not add to 1 since N_2 , which is used as a diluent, is not shown.

equilibrium if CH_4 is included in the products, as shown in figure 2(a).

Excluding CH_4 from equilibrium calculations (figure 2(b)) gives significant H_2 , the fuel for a PEM fuel cell. Therefore, one would like to achieve conditions such that CH_4 formation is suppressed. Using an integrated reactor combining POX, WGS and PROX at millisecond contact-times, we can approach the mole fractions depicted in figure 2(b). The points shown in figure 2(b) represents experimentally measured mole fractions for each of the species at the exit of each of the three stages. These mole fractions are estimated using experimental conversions in each stage individually using simulated feed from the previous stage (Rh catalyst for POX [4], Pt-tercia catalyst for WGS [8] and Ru catalyst for PROX).

Preferential oxidation of CO in a large excess of H_2 ($H_2/CO = 50$, achieved in short contact-time WGS stage) requires a catalyst that reacts O_2 with CO while inhibiting the very fast surface reaction with H_2 . This requires blocking surface sites towards adsorption of H_2 , and at low temperatures ($T = 150\text{--}200\text{ }^{\circ}C$) this occurs by competitive adsorption of CO which is more strongly bound than H_2 on noble metal surfaces. In this research, we

show that the presence of H_2O also blocks H_2 adsorption which allows reaction at higher temperatures where reaction rates are much higher to permit complete reaction in ~ 15 ms.

PROX of CO has been studied on a wide variety of catalysts on numerous supports at a multitude of conditions. These studies indicate that noble metals such as Pt [9–25,34], Rh [14,16,23,26], Ru [14,22,23,27–31] and Au [32,33] provide high CO conversion and high oxygen selectivity for CO.

Pt is the most studied catalyst for PROX of CO [9–25,34]. One of the earliest studies of CO oxidation using noble metal catalysts was conducted by Oh and Sinkevitch [14] who studied the reaction on a number of noble metals (Pt, Rh, Ru, Pd) supported Al_2O_3 catalysts between 50 and 400 $^{\circ}C$ and reported the following CO oxidation activity: $Ru > Rh > Pt > Pd$. Manasilp and Gulari [15] reported a significant positive order in water vapor and negative order in CO_2 and proposed that the enhancement was due to the participation of hydroxyl groups formed by the dissociative adsorption of H_2O on Pt and the detrimental effect of CO_2 was attributed to the RWGS reaction.

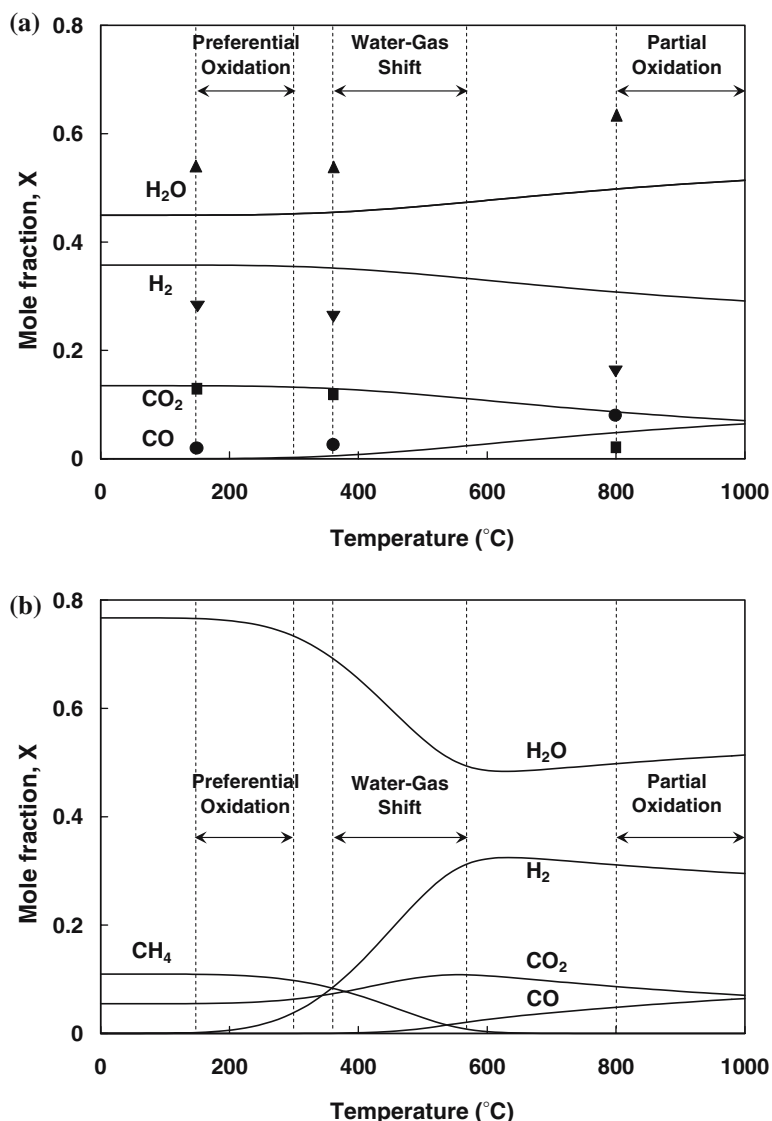


Figure 2. Equilibrium mole fraction profiles for different species as a function of temperature (a) with CH_4 , (b) without CH_4 in the products. The feed for (a) consists of 0.72 CH_4 , 0.48 O_2 , 2.88 H_2O and 0.3 N_2 and the feed for (b) consists of 0.48 CO , 0.24 CO_2 , 1.44 H_2 , 2.88 H_2O and 0.3 N_2 (all in standard liters per minute). The points in (b) show the measured values of mole fractions of different species in our short contact-time reactor estimated using experimental conversions in each stage individually using simulated feed from the previous stage.

Farrauto and coworkers [11,12] examined CO oxidation on oxide-promoted Pt catalysts. They observed low temperature (30–90 °C) CO conversion on Fe oxide-promoted Pt catalysts and proposed that the enhancement in CO conversion was due to a dual site non-competitive mechanism in which Fe oxide provides oxygen to adsorbed CO on Pt surfaces. Water pretreatment of Pt/ Al_2O_3 catalysts has been found to enhance CO oxidation when compared with an untreated catalyst in the temperature range 27–200 °C due to smaller size of the Pt particles on the pretreated catalyst [10].

Effect of ceria on Pt catalyst for CO oxidation has also been studied widely due to the oxygen-storage properties of ceria [13,21,25,34]. Significant enhancement in CO conversion and selectivity on the

ceria-promoted catalyst has been attributed to the ability of ceria to supply oxygen to Pt and suppress H_2 oxidation [13,34].

Echigo *et al.* [27–29] reported that the performance of Ru/ Al_2O_3 catalyst was improved when the catalyst was activated in a H_2/N_2 atmosphere at 250 °C for 2 h, but this also led to more methanation at temperatures above 140 °C. A negative reaction order of -0.48 for CO and 0.85 for O_2 was reported for the Ru catalyst by Han *et al.* and found to be consistent with the low-rate Langmuir–Hinshelwood reaction mechanism where CO and H_2 oxidation were limited by a CO adalayer [23,31]. The negative order for CO is supported by the power law expression proposed for Pt catalyst [9]. Han *et al.* [23] compared Rh/MgO with Ru/ $\gamma-Al_2O_3$ and Pt/ $\gamma-Al_2O_3$ for CO oxidation using a 1% CO, 65% H_2 , 10%

H₂O and balance CO₂ feed at temperatures between 50 and 350 °C and reported that Rh/MgO could be operated at ~250 °C without methanation or RWGS.

Most of these previous studies employed long residence times to achieve high conversions, and/or had a feed that did not contain CO₂ and/or H₂O, and the catalysts required elaborate preparation procedures before use. Excess H₂ and absence of H₂O in some studies precludes the possibility of CO conversion through WGS while absence of CO₂ rules out methanation reaction between H₂ and CO₂.

It is the intent of this paper to examine the preferential oxidation of CO at very short contact times (~10–15 ms) in a temperature range 150–500 °C using a simulated feed which represents the WGS product stream containing air as the source of oxygen. These experiments therefore incorporate the roles of forward and reverse WGS and methanation reactions at these conditions.

2. Experimental

For all experiments, low-surface area (nominal BET surface area ~5 m²/g, pore volume ~0.18 cc Hg/gm), 1.3 mm diameter alumina spheres were used. The spheres were coated with metal using an aqueous solution of metal salts (H₂PtCl₆, Rh(NO₃)₃, Pd(NO₃)₂, RuCl₃). The metal salt solution was dripped on to the spheres repeatedly, allowing the water to evaporate between applications. The coated spheres were then calcined at 400 °C for 5 h in a closed furnace. In each case, a calculated amount of metal salt was used to ensure 5 wt.% metal loading based on the mass of the spheres. For Pt-ceria catalyst, ceria was added to the spheres before Pt using an aqueous solution of Ce(NO₃)₃ followed by heating at 400 °C for 5 h in a closed furnace.

The experiments were carried out in a tube furnace to avoid condensation of steam in the reactor. The reactor was an 18 mm diameter quartz tube in which a sphere bed of catalyst 3.5 cm long (~7.9 cm³ of catalyst) was contained using alumina foam monoliths at both ends. The monoliths and the sphere bed were sealed into the reactor using alumina cloth.

The feed to the reactor was a simulated WGS product stream to which air was added to provide O₂ needed for the reaction. For all experiments, the total reactant flow was 5 SLPM with 17% N₂, 0.5% CO, with or without 0.25% O₂ (0.5% CO with 0.25% O₂ corresponds to CO/O₂ = 2/1 which is the stoichiometric amount of O₂ needed to oxidize CO). In one set of experiments 50% steam was used in the feed with 23% H₂ and 9.25% CO₂ (H₂/CO₂ = 2.5). For a feed with 25% steam, the corresponding H₂ and CO₂ were 40.90% and 16.35%, respectively (H₂/CO₂ = 2.5). Steam was generated in a heater at approximately 600 °C and the rate of steam

generation was controlled using syringe pump. The flow of gases was controlled using mass flow controllers and all the gases and steam were delivered through a tube wrapped in heating tape prior to being fed to the reactor.

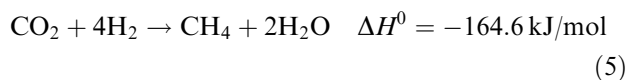
The experimental procedure consisted of heating the furnace to ~500 °C and reducing the temperature in steps until negligible CO conversion was observed. The reactor temperature was always kept above 150 °C to prevent the condensation of steam on the catalyst. For all experiments, the temperatures were measured at the outlet of the catalyst bed. Gas samples were taken through a septum at the exit of the reactor using a gas tight syringe and analyzed in a gas chromatograph equipped with a thermal conductivity detector. Mass balances in carbon typically closed within ±5%. All catalysts were used for at least 20 h at different temperatures with no hysteresis or deactivation detected.

3. Results and discussion

Many different reactions become important at the temperatures and feed compositions in our system and, consequently, there are different ways in which CO is consumed in our system. Apart from WGS and PROX reactions, CO can be consumed in our system in the methanation reaction 1 (MR1)



We designed the experiments so that we could estimate CO conversion exclusively due to PROX and thus distinguish it from CO conversion obtained as a result of WGS and MR1 reactions. When our feed contains O₂, WGS, PROX and MR1 reactions occur on the catalyst. When there is no O₂ in the feed, on the other hand, PROX cannot occur and CO conversion in the system is due to WGS and MR1 reactions. It should be noted that WGS is reversible at our reaction conditions and, therefore, we can have CO production (reverse WGS) in our system. Negative CO conversions shown in the results are due to this reaction. Another reaction which does not consume CO but which is possible at these conditions is the CH₄ synthesis reaction from CO₂ and H₂



Though this reaction is a combination of two reactions (it can be obtained by adding the reverse of WGS to MR1), we will consider it as a single reaction for the results we present and refer it to as methanation reaction 2 (MR2).

While we are primarily concerned with CO removal in our system, we also consider methanation reactions since they lead to the loss of H₂ in our system. Our goal is to find suitable catalysts and conditions at which we

get high selectivity for CO oxidation and low selectivity for CH_4 formation.

Figure 3(a) shows CO conversions obtained on different catalysts as a function of temperature for a feed containing 25% steam (17% N_2 , 0.5% CO, 0.25% O_2 , 40.9% H_2 and 16.35% CO_2). Equilibrium CO conversion at these conditions is also shown for comparison. Except equilibrium, all the curves show a maximum in CO conversion. To the right of the maxima, CO conversion decreases due to H_2 oxidation and RWGS while to the left, the decrease is due to very low CO oxidation rates at the low temperatures. Ru and Rh give CO

conversions of greater than 80% at temperatures of 300 °C; Pt and Pt-ceria give highest CO conversions of 50% at temperatures of 250 °C, while Pd gives CO conversions of less than 20% at all temperatures. Though not shown here, O_2 conversion was $\sim 100\%$ at all feed and reactor conditions for Rh, Ru and Pd catalysts while it varied between 40% and 100% for Pt and Pt-ceria catalysts. Therefore, O_2 selectivity of CO for Rh, Ru and Pd catalysts is the same as CO conversion.

As noted above, WGS, MR1 and MR2 reactions can occur at these conditions. To estimate the extent of these reactions, we repeated the above set of experiments on

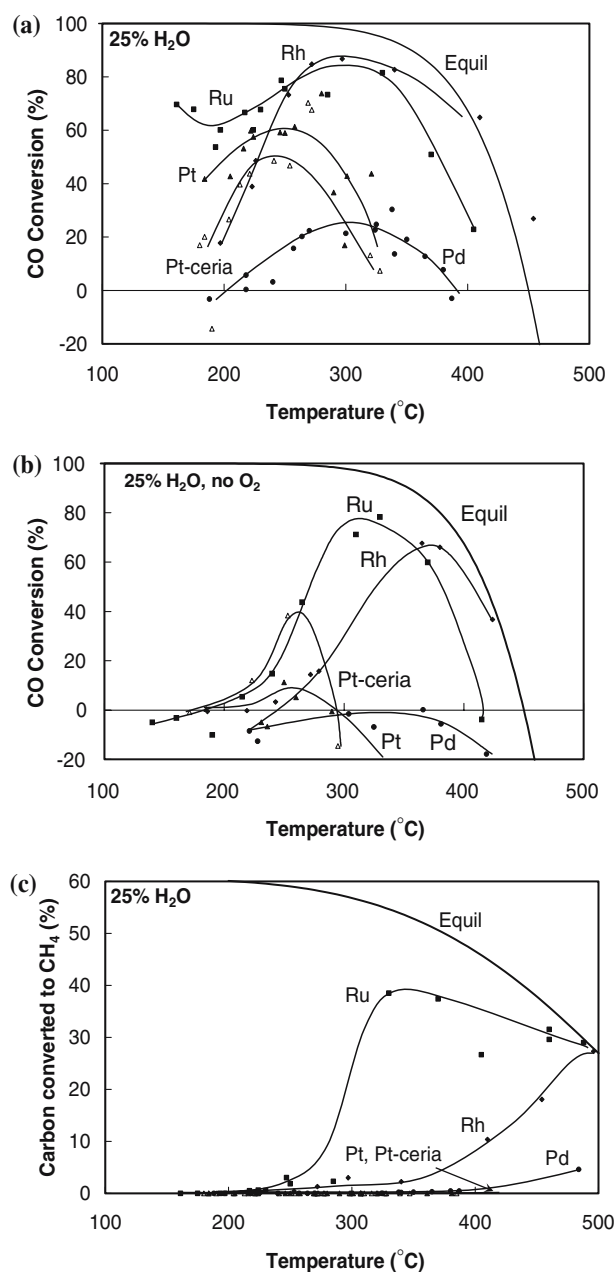


Figure 3. Measured CO conversion on different catalysts (with 25% H_2O in the feed) as a function of temperature for a feed containing 0.5% CO, 17% N_2 , 40.9% H_2 and 16.35% CO_2 (a) in the presence of stoichiometric amount of O_2 (0.25%), (b) in the absence of O_2 and (c) percent carbon converted to CH_4 in the presence of O_2 .

the same catalysts with the same feed except that O_2 was now removed from the feed. The results are shown in figure 3(b). It is clear from these results that Pt and Pd do not show significant extent of WGS and MR1. In fact, we can see negative CO conversions for Pd implying that RWGS occurs at these conditions. For Ru, Rh and Pt-ceria, high CO conversions imply that WGS and MR1 reactions occur to a significant extent. To distinguish between these two reactions, we plot the percent of carbon that is converted to CH_4 in figure 3(c). It should be noted that figure 3(c) presents the results for a feed that contained O_2 since the percent of carbon

converted to CH_4 was always higher for the feed that contained O_2 as compared to the feed not containing O_2 . Since Pt-ceria catalyst forms no CH_4 , therefore, CO conversion shown in figure 3(a) is due to the WGS. Ru and Rh, on the other hand, produce a significant amount of CH_4 at temperatures greater than 250 and 350 $^{\circ}C$, respectively. The only sources of carbon in our feed are CO and CO_2 and the relative amount of carbon from CO is 2.9% (amount of carbon from CO/(amount of carbon from CO + CO_2)). Since we observe more than 20% carbon conversion to CH_4 on Rh and Ru, most of the CH_4 forms *via* MR2.

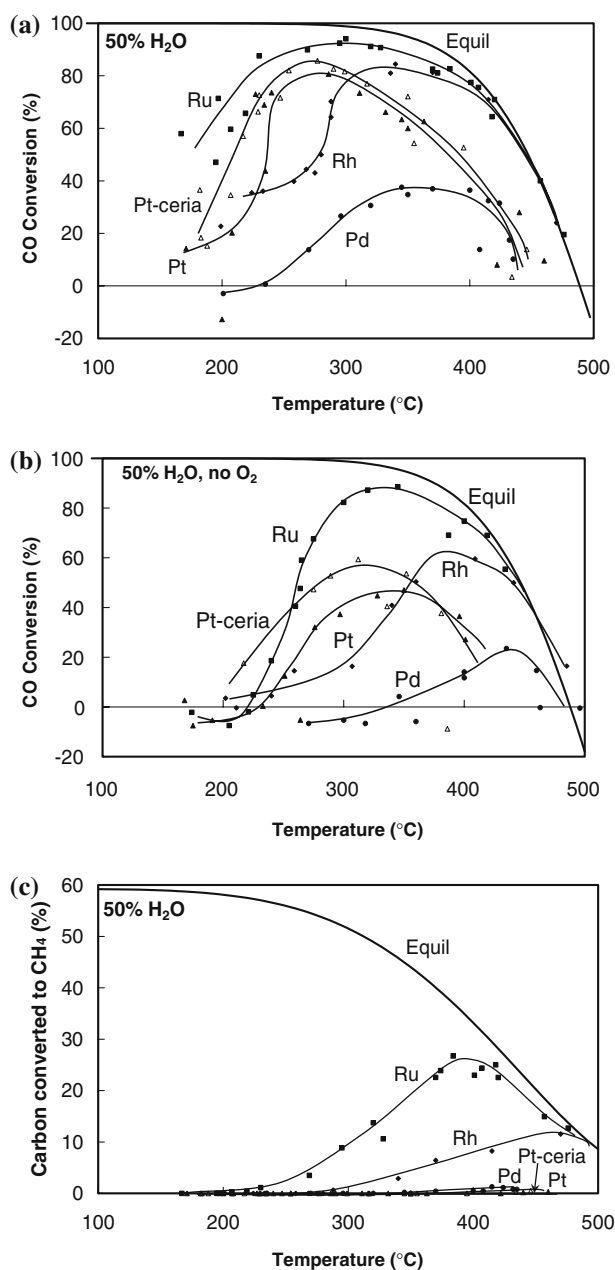


Figure 4. Measured CO conversion on different catalysts (with 50% H_2O in the feed) as a function of temperature for a feed containing 0.5% CO, 17% N_2 , 23% H_2 and 9.25% CO_2 (a) in the presence of stoichiometric amount of O_2 (0.25%), (b) in the absence of O_2 and (c) percent carbon converted to CH_4 in the presence of O_2 .

From the results of figure 3(a)–(c), it is clear that Ru is a good PROX catalyst at temperatures less than 250 °C while Rh gives high CO conversions at temperatures between 250 and 400 °C.

We also performed experiments with a feed containing 50% steam (17% N₂, 0.5% CO, 0.25% O₂, 23% H₂ and 9.25% CO₂) to examine the effect of high water content on PROX of CO. Figure 4(a)–(c) presents the results for these experiments. A comparison of figures 3(a) and 4(a) show that Pt and Pt-ceria give 30% additional conversion with feed containing higher steam content (CO conversion on Pt increases from 50% to 80% at 250 °C when the steam content of the feed is increased from 25% to 50%). For Rh, Ru and Pd, there is a very small increase in CO conversion. Results from figure 4(b), which presents the results for feed with no O₂, can be compared with those from figure 4(a) to estimate the extent to which PROX is responsible for CO conversion at these conditions. With higher steam content in the feed, WGS occurs to a higher extent and at higher temperatures on all catalysts. Pt and Pd show the maximum increase in WGS activity. While Pd gave negative CO conversions at all temperatures with 25% steam, it gives 20% CO conversion at 450 °C with 50% steam (figure 4(b)). Similarly Pt, which gave less than 10% CO conversion with 25% steam and no O₂, gives 40% CO conversion in a wide temperature range with 50% steam in feed. Higher steam content also suppresses CH₄ formation as can be seen from a comparison of figures 3(c) and 4(c) which plot the percent of carbon converted to CH₄ for different catalysts. The maximum CH₄ formation on Ru drops from a value of 40% to less than 30% as the steam content of the feed stream is increased from 25% to 50%.

The above results indicate the following order for CO oxidation on different catalysts between 200 and 400 °C: Ru > Rh > Pt > Pd. Oh and Sinkevitch [14] reported the same order with a different feed (it did not contain CO₂ and H₂O) while Han *et al.* [23,31] reported similar CO conversions on Rh and Ru catalysts at lower temperatures with a feed containing CO₂ and H₂O. We see no enhancement in CO conversion due to the presence of ceria as reported by other researchers [13,34]. In fact, Pt-ceria gives lower conversion than Pt catalyst (figure 3(a)) indicating that ceria suppresses CO oxidation. Further, higher CO conversion on Pt-ceria as compared to Pt for feed without O₂ (figures 3(b) and 4(b)) indicates that ceria promotes WGS as reported in an earlier study [8].

From the above results, we also see a strong effect of water in terms of increased WGS activity and suppression of methanation activity as well as suppression of H₂ oxidation. Similar but less pronounced observations have been reported by other researchers [15,16,28]. It is hypothesized that hydroxyl group formed on the catalyst due to adsorption of water is a better oxidant than oxygen and increases the oxidation rate of CO and H₂ [15]. Choi *et al.* [16] reported positive effect of water for

temperatures up to 220 °C, while above 220 °C, only large amounts of water (>15%) had positive effect while smaller amounts of water were detrimental.

4. Summary

These results show that high CO conversions (~90%) can be achieved on Rh and Ru catalysts at ~15 ms contact times at temperatures less than 300 °C for a feed containing 0.5% CO using stoichiometric amounts of O₂ (0.25%). The effect of varying H₂O, H₂ and CO₂ in the feed stream show that a higher steam content (50%) in the feed leads to significant WGS on Pt and Pt-ceria, and suppresses CH₄ formation on Ru, Rh and Pd. The results also show that Ru and Rh give significant methanation at temperatures greater than 250 and 350 °C, respectively. From these results we conclude that PROX occurs on Ru (giving CO conversions between 60% and 85%) at temperatures less than 250 °C without any other side reactions like water-gas shift and methanation. On Rh, PROX can be carried out with 80% CO conversion at temperatures between 275 and 350 °C. A multistage reactor incorporating these catalysts can be used to bring down CO concentration from 5000 ppm (0.5%) to less than 100 ppm.

References

- [1] C. Song, *Catal. Today* 77 (2002) 17.
- [2] T.V. Choudhary and D.W. Goodman, *Catal. Today* 77 (2002) 65.
- [3] A.F. Ghenciu, *Curr. Opin. Solid State Mater. Sci.* 6 (2002) 389.
- [4] D.A. Hickman and L.D. Schmidt, *Science* 259 (1993) 343.
- [5] J.J. Krummenacher, K.N. West and L.D. Schmidt, *J. Catal.* 215 (2003) 332.
- [6] E.C. Wanat, K. Venkataraman and L.D. Schmidt, *Appl. Catal. A* 276 (2004) 155.
- [7] R. Subramanian, G.J. Panuccio, J.J. Krummenacher, I.C. Lee and L.D. Schmidt, *Chem. Eng. Sci.* 59 (2004) 5501.
- [8] C. Wheeler, A. Jhalani, E.J. Klein, S. Tummala and L.D. Schmidt, *J. Catal.* 223 (2004) 191.
- [9] D.H. Kim and M.S. Lim, *Appl. Catal. A* 224 (2002) 27.
- [10] I.H. Son, M. Shamsuzzoha and A.M. Lane, *J. Catal.* 210 (2002) 460.
- [11] O. Korotkikh and R. Farrauto, *Catal. Today* 62 (2000) 249.
- [12] X. Liu, O. Korotkikh and R. Farrauto, *Appl. Catal. A* 226 (2002) 293.
- [13] I.H. Son and A.M. Lane, *Catal. Lett.* 76 (2001) 151.
- [14] S.H. Oh and R.M. Sinkevitch, *J. Catal.* 142 (1993) 254.
- [15] A. Manasilp and E. Gulari, *Appl. Catal. B* 37 (2002) 17.
- [16] Y. Choi and H.G. Stenger, *J. Power Sources* 129 (2004) 246.
- [17] M. Watanabe, H. Uchida, H. Igarashi and M. Suzuki, *Chem. Lett.* 25 (1995).
- [18] H. Igarashi, H. Uchida, M. Suzuki, Y. Sasaki and M. Watanabe, *Appl. Catal. A* 159 (1997) 159.
- [19] C. Kwak, T.J. Park and D.J. Suh, *Chem. Eng. Sci.* 60 (2005) 1211.
- [20] C. Kwak, T.J. Park and D.J. Suh, *Appl. Catal. A* 278 (2005) 181.
- [21] F. Marino, C. Descorme and D. Duprez, *Appl. Catal. B* 54 (2004) 59.
- [22] H. Igarashi, H. Uchida and M. Watanabe, *Chem. Lett.* 1262 (2000).
- [23] Y.F. Han, M.J. Kahlich, M. Kinne and R.J. Behm, *Appl. Catal. B* 50 (2004) 209.

- [24] G.W. Roberts, P. Chin, X. Sun and J.J. Spivey, *Appl. Catal. B.* 46 (2003) 601.
- [25] D. Tibiletti, E.A.B. de Graaf, S.P. The, G. Rothenberg, D. Farrusseng and C. Mirodatos, *J. Catal.* 225 (2004) 489.
- [26] S.H. Oh, G.B. Fisher, J.E. Carpenter and D.W. Goodman, *J. Catal.* 100 (1986) 360.
- [27] M. Echigo, N. Shinke, S. Takami and T. Tabata, *J. Power Sources* 132 (2004) 29.
- [28] M. Echigo and T. Tabata, *J. Chem. Eng. Japan* 37 (2004) 558.
- [29] M. Echigo and T. Tabata, *Appl. Catal. A* 251 (2003) 157.
- [30] S. Kawatsu, *J. Power Sources* 71 (1998) 150.
- [31] Y.F. Han, M.J. Kahlich, M. Kinne and R.J. Behm, *Phys. Chem. Chem. Phys.* 4 (2002) 389.
- [32] M. Okumura, S. Nakamura, S. Tsubota, T. Nakamura, M. Azuma and M. Haruta, *Catal. Lett.* 51 (1998) 53.
- [33] M.M. Schubert, M.J. Kahlich, H.A. Gasteiger and R.J. Behm, *J. Power Sources* 84 (1999) 175.
- [34] H.S. Roh, H.S. Potdar, K.W. Jun, S.Y. Han and J.W. Kim, *Catal. Lett.* 93 (2004) 203.